Coronal mass ejections: a driver of severe space weather

Lucie Green and Deb Baker
Mullard Space Science Laboratory, UCL

Introduction

Observational studies of the solar atmosphere in the early 1970s revealed that the Sun sporadically ejects vast quantities of matter into the Solar System in addition to the constant outflow known as the solar wind (Tousey, 1973). These sporadic ejections are known today as coronal mass ejections (CMEs). They are seen in images that use an occulting disc to block the dazzling light emitted by the photosphere, creating an artificial solar eclipse and allowing the outer atmosphere to be viewed (Figure 1). CMEs are then revealed as outward moving structures that exhibit a range of morphologies and which carry around 10^{12}kg of magnetised plasma into the heliosphere with an average speed of ~490kms^{-1} (Webb and Howard, 2012). Upon eruption, these magnetic structures quickly expand to become larger than the Sun itself.

CMEs are common events and occur with a frequency that follows the (on average) 11-year solar cycle with approximately one CME being formed per day at cycle minimum and as many as five per day at cycle maximum (Webb and Howard, 2012). The solar cycle is driven by an evolving global magnetic field that changes in strength and complexity and which manifests itself in the photosphere by the presence of sunspots – regions of concentrated magnetic field. As the solar cycle ebbs and flows, the magnetic field in the solar atmosphere is transformed between a magnetically simple state when there are correspondingly few sunspots at the surface, and a magnetically complex configuration when there are many sunspots. In this way, CMEs can be understood as a mechanism by which the Sun ejects atmospheric magnetic field that harbours both magnetic energy and a complex morphology (Low, 1996). CMEs play an important role in the magnetic cycle of the Sun. For recent review articles on CMEs see, for example, Webb and Howard (2012), Chen (2011) and Forbes *et al*. (2006).

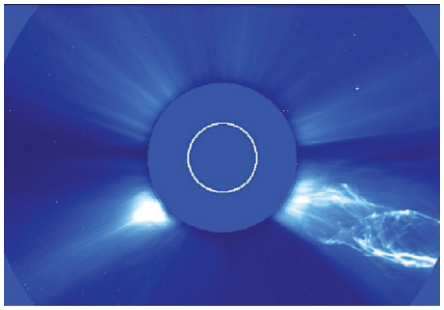

Figure 1. A SOHO/LASCO image of a coronal mass ejection that occurred on 2 June 1998. The erupting structure is seen in the lower right and exhibits a twisted or helical shape. The white circle indicates the size of the solar disc; the size of the occulting disc is shown by the blue filled circle. The SOHO spacecraft is located at the L1 position. (Image courtesy of ESA/NASA - http://sohowww.nascom.nasa.gov/gallery/images/c2helix.html)

CMEs and their relevance to space weather

The discovery of CMEs goes beyond elucidating important aspects of the Sun's magnetic field evolution. The discovery of these ejections answered an outstanding question in solar-terrestrial physics when it was realised that they are the solar phenomenon that are the cause of major, but transient, disturbances to the geomagnetic field (e.g. Gosling, 1993). When CMEs collide with the Earth's magnetic field (the magnetosphere) they can compress its dayside and, if the magnetic field of the CME is of the correct orientation, magnetic reconnection between the CME and the magnetosphere can occur. Magnetic reconnection is a fundamental physical process in which plasma and magnetic field become momentarily decoupled, leading to a reconfiguration of the field and the conversion of magnetic energy into other forms of energy. The magnetic field at the sub-solar point of the magnetosphere (directly between the Sun and the Earth) is strongly northward, so a strong southward directed magnetic field within the CME could lead to magnetic reconnection and a joining of the magnetic field of the CME with the magnetosphere. If this occurs, the dayside magnetospheric flux gets dragged over to the nightside by the motion of the CME, and an accumulation of magnetic flux then occurs in this part of the magnetosphere, followed by magnetic reconnection. This reconfiguration of the nightside magnetosphere allows magnetic flux to move back to the dayside, where it can undergo reconnection with the CME once again. This process is known as the Dungey cycle (Dungey, 1961). During these times the magnetosphere is driven into a disturbed state, producing geomagnetic sub-storms and storms which then lead to a multitude of space weather effects (Pulkkinen, 2007).

CMEs, which are the bulk ejection of magnetised plasma, are often temporally and spatially associated with another form of solar activity known as a solar flare – sudden bursts of electromagnetic radiation (decametre radio waves to gamma-rays) and high-energy particles (Benz, 2008). This CME-flare association has its origins in the physical processes that are common to both phenomena. Solar flares arise from the conversion of magnetic energy into other forms during magnetic reconnection, and this energy conversion leads to the production of electromagnetic radiation. However, magnetic reconnection also reconfigures the magnetic field during a CME, which accelerates the magnetised plasma away from the Sun. Despite these common aspects, CMEs and flares are very distinct in terms of their physical guise. Solar flares have a space weather impact through their high-energy radiation that ionises the Earth's upper atmosphere, and through the protons that are accelerated to near-relativistic energies, posing a threat to spacecraft and humans in space.

Extreme space weather events

The most extreme space weather event in our records is the geomagnetic storm that began on 2 September 1859 (Tsurutani *et al*., 2003). This storm has become known as the Carrington event, named after the Victorian amateur astronomer who observed the associated flare, which occurred in a

large sunspot group he was drawing at his observatory in Redhill (Surrey). Less than a day later, an intense display of the aurora erupted, which was seen down to exceptionally low latitudes as an intense geomagnetic storm took hold. Measurements from a magnetometer in Bombay, India, revealed the exceptional changes to the Earth's magnetic field that occurred (Siscoe *et al*., 2006). The significant aspect of this event, which was unknown to Carrington at the time, was that the sunspot group had produced a CME at the same time as the flare. The CME reached the Earth after only 17.5h, giving it a mean velocity along the Sun–Earth line of ≈2300kms^{-1}. The most intense geomagnetic storms (Gonzalez *et al*., 1994) are associated with CMEs that have a large velocity as this can lead to a large inflow of magnetic flux. Multiple CMEs may also be important as earlier eruptions could create the solar wind conditions necessary for a subsequently fast CME. It looks likely that the Carrington CME occurred at a time of heightened solar activity, and the geomagnetic records suggest another CME had occurred just a few days before (Boteler, 2006).

Intense geomagnetic storms are also related to CMEs that have a high dynamic pressure as this leads to a high momentum flux (Svalgaard, 1977). The great geomagnetic storm of 13 March 1989 (Allen *et al*., 1989) is an example of an extreme geomagnetic storm that was driven by a CME that was not exceptional in terms of its velocity; its mean Sun-Earth transit time was 770kms^{-1} (Feynman and Hundhausen, 1994). However, Feynman and Hundhausen (1994) remark that the CME was *exceptionally bright* in the coronagraph data, which strongly supports an interpretation that it was a very massive eruption (the coronagraph images detect photospheric light scattered by coronal electrons, and brightness is therefore a function of density) and therefore could have had a high dynamic pressure when it reached the magnetosphere. Indeed, the dayside magnetosphere is thought to have been compressed towards the Earth, by more than a factor of two, for an extended period of time (Allen *et al*., 1989). In addition to the above, it is possible that the pre-existing condition of the magnetosphere plays a role in severe geomagnetic storms. There are studies that indicate preconditioning may not play a significant role in strengthening the storm intensity, but it may lengthen the storm duration (e.g. Xie *et al*., 2008).

The factors that are important for a geo-effective CME are the strength of the southward magnetic field component (B_z), the velocity of the solar wind (V_{sw}) and the solar wind dynamic pressure (ρV_{sw}):

$$B_z\, V_{sw}\, (\rho V_{sw})$$

One thing remains clear though: the most intense geomagnetic storms will not be triggered unless the CME has the correct magnetic field configuration. Intense geomagnetic storms require the presence of a strong southward magnetic field component more than any other plasma parameter, (Gonzalez *et al*., 2011) and this southward field must persist for several hours (Russell *et al*., 1974). This is because the strong southward component provides an effective coupling of the magnetic field of the CME with the magnetosphere, which controls the transfer of energy. NASA's ACE spacecraft at the first Lagrange point constantly monitors this magnetic field component, 1.6 million km upstream of the Earth. It is referred to as the B_z component as its axis is parallel to the ecliptic pole in the Geocentric Solar Ecliptic coordinate system.

Predicting extreme space weather

The role of CMEs in driving extreme geomagnetic activity has led to efforts in both modelling and observation to predict their velocity and arrival times at Earth. During their eruption, CMEs are rapidly accelerated at low altitudes in the solar atmosphere to velocities across a broad range from 100kms^{-1} to more than 3000kms^{-1}. The travel time of CMEs from the Sun to 1AU (1AU is the astronomical unit for the Sun-Earth distance) varies from less than 24h to more than 3 days; a surprisingly small range, given the distribution of initial velocities. This is explained by the fastest CMEs being decelerated in the solar wind (Woo *et al*., 1985; Watari and Detman, 1998) and the slower ones being accelerated by the solar wind flow (Lindsay *et al*., 1999) so that by the time CMEs arrive at 1AU the majority are travelling at a speed close to that of the ambient solar wind flow (between 350 and 550kms^{-1}, Gopalswamy *et al*., 2000). So, for an extreme event the CME needs to have a high velocity at 1AU, which means it needs to have a high velocity when leaving the Sun and experience a low aerodynamic drag force in the solar wind. In addition, it needs to hit the magnetosphere head-on (i.e. not give us a glancing blow), have a high dynamic pressure and have a magnetic configuration with a strong and sustained southward component. It is this combination of factors that needs to be accurately identified in a CME from the plethora that leave the Sun.

The propagation time of CMEs means that forecasting their occurrence may not necessarily be required. In the majority of cases, space weather users have upwards of a day to make their preparations once an eruption has been observed. Once a CME has been observed, models exist to forecast the direction of propagation and, if Earth-directed, the CME arrival time at 1AU (Cargill and Schmidt, 2002; Owens and Cargill, 2004). However, for a Carrington-type event the CME transit timescale may well be insufficient for producing a timely forecast once the delay in receiving the observational data has been factored in. In light of this, attempts are being made to determine the likelihood of a CME occurring in the solar atmosphere based on observations. A brief summary of eruptive indicators and time scales is given in Table 1.

Currently, the longest observational warning of an Earth-directed CME occurrence is provided by the presence of a so-called sigmoid – an S-shaped structure seen in soft X-ray or EUV images of the solar atmosphere (Canfield *et al*., 1999). Once this shape is seen, the region is likely to erupt within hours (i.e. not days) (Green and Kliem, 2014). Due to projection effects, these features are best seen when the magnetic configuration is viewed from above, that is, when they are near Sun centre. Eruptions from these features are therefore likely to be Earth-directed. This is in contrast to another observational indicator of an ensuing CME, namely streamer blowouts, which are seen on the solar limb and are not so likely to be Earth directed.

Identifying and modelling the pre-eruption magnetic configuration of sigmoids using solar observations raises the opportunity of inserting this magnetic configuration

Table 1

Summary of the three main observational indicators that a CME is likely to happen along with their timescales.

Solar feature	*Eruption indicator*	*References*
Filament: observed anywhere on the Sun	Filaments darken and broaden tens of minutes prior to their eruption.	Martin (1980)
Streamer: observed at the limb only	Streamers brighten over one to several days before eruption. They often also include a filament eruption.	Sheeley *et al.* (1982) and Illing and Hundhausen (1986)
Sigmoid: most easily observed near Sun centre	Their appearance precedes an eruption by a few hours.	Canfield *et al.* (1999) and Green and Kliem (2014)

into the propagation models mentioned above and eventually achieving data-driven simulations of CMEs from Sun to Earth in the coming years. It is also worth noting that, since there is a close association between CMEs and solar flares, the use of sigmoids to predict the occurrence of an eruption is also applicable to efforts in the area of flare forecasting.

There is currently a major gap in our forecasting capability though. We still do not have a model that uses solar observations to build a realistic magnetic configuration of a CME as it leaves the Sun. Such a model would enable us to understand CME evolution through the inner heliosphere and therefore forecast the strength of the B_z field component at 1AU. This is the current space weather challenge. However, the first steps towards achieving this have been taken in fundamental solar and solar-terrestrial research.

Understanding the magnetic configuration of CMEs

When CMEs are observed *in situ* in the inner heliosphere they often exhibit a coherent structure in the solar wind that has an increased magnetic field strength as compared to the ambient solar wind flow, an anomalously low proton and electron temperature, and a large magnetic field rotation that is indicative of a particular configuration containing twisted, or helical, magnetic field known as a flux rope (Burlaga *et al*., 1981; Klein and Burlaga, 1982; Cane and Richardson, 2003). Figure 1 shows a CME whose plasma density distribution strongly supports such a twisted configuration. Indeed, it seems that most CMEs may be well modelled by a flux rope magnetic configuration regardless of their source region (Jian *et al*., 2006). This has motivated a search for flux ropes in the solar atmosphere, prior to their eruption as a CME. If found, the global aspects of their magnetic field can be studied to obtain an indication of the CME's geo-effectiveness from the orientation of the flux rope axis and the organisation of the twist, leading to a forecast of the presence of a southward-directed (B_z) magnetic field. We note that CMEs may develop sub-structure *en route* to the Earth (Steed *et al*., 2011), but this level of complexity is beyond the scope of current forecasting activity.

There is increasing evidence that magnetic flux ropes are indeed present in the solar atmosphere before CME onset, perhaps unsurprisingly in the S-shaped (sigmoidal) regions that are highly eruptive (Green and Kliem, 2009; 2014; Liu *et al*., 2010; Green *et al*., 2011; Zharkov *et al*., 2011). The three-dimensional structure of the coronal field is not directly measurable, but the flux rope configuration can be inferred from observations of the solar atmosphere in soft X-ray and EUV emission. This identification allows us to make a direct link between the CME at the Sun and the flux rope measured in situ at 1AU. The eruption of a flux rope in the solar atmosphere is another key focus of CME research. Their loss of equilibrium due to an ideal magnetohydrodynamic instability, catastrophe or force imbalance has so far been well studied and modelled in the idealised case (e.g. Hood and Priest, 1981; Forbes and Isenberg, 1991; Kliem and Török, 2006; Mackay and van Ballegooijen, 2006; Démoulin and Aulanier, 2010). Simulations of the formation of an idealised flux rope and its subsequent eruption have also been achieved (Amari *et al*., 2010; Aulanier *et al*., 2010).

Observations of flux ropes prior to their eruption are crucial for future space weather forecasting as they can be used as the input to create more realistic data-driven CME simulations. Flux ropes are modified during their eruption as this involves magnetic reconnection within the overlying/surrounding magnetic field. This reconnection adds more magnetic flux to the rope, cuts the tethers of the overlying and constraining field, and aids the acceleration of the rope away from the Sun. It is this field that forms the external field of the rope (which is likely to be more twisted than the core) and which also needs to be known to forecast its coupling to the magnetosphere. Therefore, solar observations during the dynamic phase of the eruption must also be captured.

Modelling magnetic flux ropes at the Sun

The starting point for a data-driven simulation is to model the magnetic flux rope before its eruption as a CME. The solar observations can be used to determine the spatial extent of the flux rope, the pre-eruptive orientation of the flux rope axis and even an estimation of the axial flux content in special cases (Green *et al*., 2011). The S-shaped nature of the magnetic configuration is highly suggestive that the flux ropes are weakly twisted structures containing, in most cases, little more than one turn in the magnetic field vector.

The solar data must then be used as the boundary condition for modelling the pre-eruption flux ropes. This has already been investigated using three approaches. First, by the flux rope insertion method (van Ballegooijen, 2004). This method inserts a flux rope into a magnetic field configuration that is extrapolated from solar observations. The location of the rope is guided by the observation of a filament – a dark and sinuous feature in the solar atmosphere. A match between the modelled magnetic structure and observed structure in the solar atmosphere is used to identify a realistic configuration. Many studies have been carried out using this technique, and they have found weakly twisted flux ropes in the pre-eruptive magnetic field (Bobra *et al*., 2008; Su *et al*., 2009; Savcheva and van Ballegooijen, 2009). Second is the approach that generates a time-series of 3D coronal magnetic field configurations using observations of the Sun's surface magnetic field (Mackay *et al*., 2011); as the magnetic field evolves, flux ropes can form (Gibb *et al*., 2014). Third, magnetic extrapolations are also used to reconstruct the magnetic field from observations of the three components of the vector magnetic field measured in the photosphere (e.g. Valori *et al*., 2012), but as yet the identification of flux ropes using this technique remains a challenge.

Case study: solar active region NOAA 9077

As an example of the promise of the above flux rope models, we briefly discuss here a CME productive region that was on the Sun during December 2007, named NOAA active region 9077. The active region was studied from its birth on the Sun until it produced a CME, allowing the formation of the flux rope to be studied in detail. The flux rope was built in three phases. Phase one is a phase of increasing shear, driven by the dispersal of the surface magnetic field and magnetic reconnection that removes magnetic flux from the surface layer, following the model of van Ballegooijen and Martens (1989). In phase two, there is an accumulation of a significant amount of flux that runs almost parallel to the line that separates the main magnetic polarities of the region. In phase three, further magnetic reconnection produces field lines that are twisted around the axial flux (which look S-shaped) and which contribute poloidal flux and define the presence of a flux rope. Images in Figure 2 show these three phases for this solar active region and three others for emphasis. The observational approach to studying the magnetic flux content of the rope was brought together with the flux rope insertion method in Savcheva *et al*. (2012), who suggested the reliability of both modelling and observational approaches. Gibb *et al*. (2014) also studied this region and managed to reproduce the main features of the magnetic field evolution including the formation of the flux rope in the correct location. Figure 3 shows the results of these three studies and directly compares the observed and modelled magnetic configurations.

The future

This paper gives a brief summary of the current status of our understanding of coronal

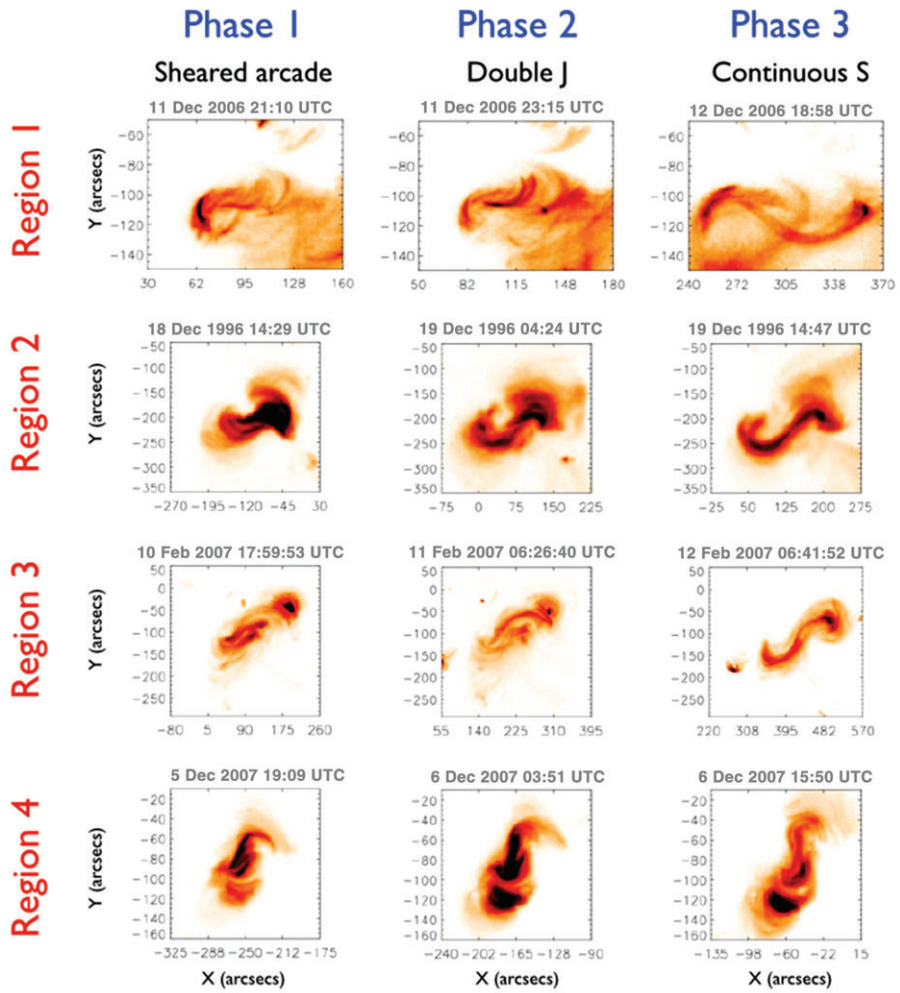

Figure 2. Hinode/XRT do X-ray images showing examples of S-shaped (sigmoidal) regions during the three phases of their evolution. Top row: NOAA region 10930. Second row from the top: NOAA region 8005. Second row from the bottom: an un-numbered region observed on the disc during February 2007. Bottom row: NOAA region 10977. (Image modified from Green and Kliem (2014).)

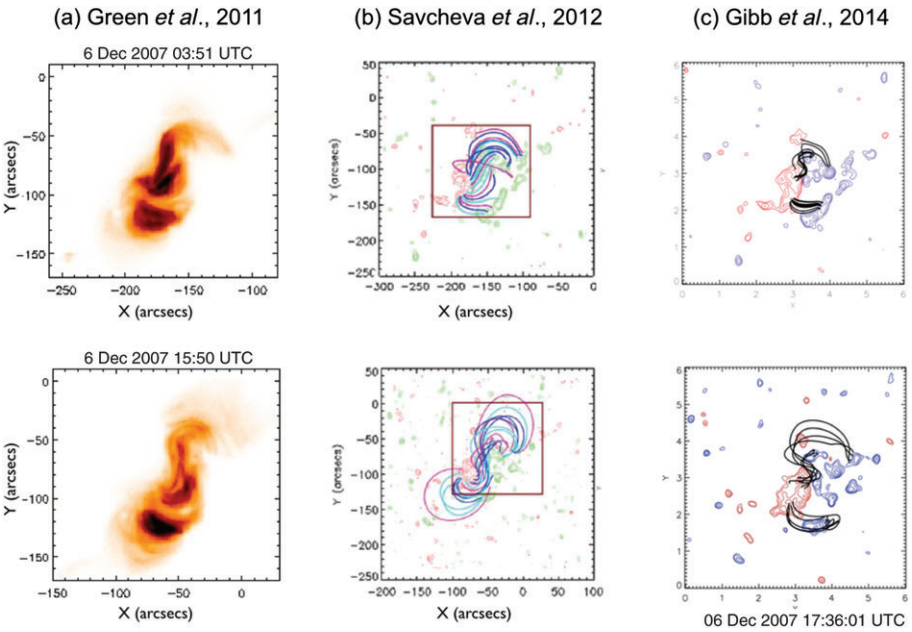

Figure 3. Comparison between observed and modelled magnetic configuration of solar active region 9077 at two different times. Columns: (a) soft X-ray emission structure observed on the Sun as shown in Green et al. (2011), (b) modelled magnetic configuration of Savcheva et al. (2012), (c) modelled magnetic configuration of Gibb et al. (2014). The observations and models suggest that a magnetic flux rope has formed by 6 December 2007 around 1550 UTC (bottom row). Note: the size scale varies between panels in the figure.

mass ejections and the importance of being able to model their magnetic configuration in order to predict severe space weather. We must develop a capability to forecast the strength of the southward magnetic field component (B_z) of Earth-directed CMEs as well as their velocity and plasma parameters. This is achievable in the near future if the developments we have made in understanding the magnetic configuration of the pre-eruption structure from solar observations, the advances in modelling the magnetic configuration before the eruption, and data-driven (meaning realistic) simulations of the eruption itself are brought together. From these areas of competency we have the opportunity to work towards two data products that would be valuable for space weather forecasting in relation to CMEs:

1. Exploitation of magnetic field extrapolations and observations of the solar atmosphere to create a near-real-time map of potential space weather 'hot spots' on the Sun. That is, where a magnetic configuration is seen to be forming which has a high likelihood of producing a CME with a strong and sustained B_z component.
2. Data-driven simulations of CMEs to produce a 'real Sun' scenario. These simulations in turn need to be coupled to heliospheric simulations that then propagate the CME configuration to 1AU.

Acknowledgements

LMG is grateful to the Royal Society for the award of a University Research Fellowship. DB acknowledges support by STFC Consolidated Grant ST/H00260/1. The authors thank Gordon Gibb for supplying a magnetic field extrapolation for Figure 3.

References

Allen J, Frank L, Sauer H *et al.* 1989. Effects of the March 1989 solar activity. *EOS Trans. AGU* **70**: 1479.

Amari T, Aly J-J, Mikic Z *et al.* 2010. Coronal mass ejection initiation: on the nature of the flux cancellation model. *Astrophys. J.* **717**: L26.

Aulanier G, Török T, Démoulin P *et al.* 2010. Formation of Torus-unstable flux ropes and electric currents in erupting sigmoids. *Astrophys. J.* **708**: 314.

van Ballegooijen AA. 2004. Observations and modeling of a filament on the Sun. *Astrophys. J.* **612**: 519.

van Ballegooijen AA, Martens PCH. 1989. Formation and eruption of solar prominences. *Astrophys. J.* **343**: 971.

Benz AO. 2008. Flare observations. *Living Rev. Sol. Phys.* **5**: 1.

Bobra MG, van Ballegooijen AA, DeLuca EE. 2008. Modeling nonpotential magnetic fields in solar active regions. *Astrophys. J.* **672**: 1209.

Boteler DH. 2006. The super storms of August/September 1859 and their effects on the telegraph system. *Adv. Space Res.* **38**: 159.

Burlaga L, Sittler E, Mariani F *et al.* 1981. Magnetic loop behind an interplanetary shock – Voyager, Helios, and IMP 8 observations. *J. Geophys. Res., Space Phys.* **86**: 6673.

Cane HV, Richardson IG. 2003. Interplanetary coronal mass ejections in the near-Earth solar wind during 1996–2002. *J. Geophys. Res., Space Phys.* **108**: 1156.

Canfield RC, Hudson HS, McKenzie DE. 1999. Sigmoidal morphology and eruptive solar activity. *Geophys. Res. Lett.* **26**: 627.

Cargill PJ, Schmidt JM. 2002. Modelling interplanetary CMEs using magnetohydrodynamic simulations. *Ann. Geophys.* **20**: 879.

Chen PF. 2011. Coronal mass ejections: models and their observational basis. *Living Rev. Sol. Phys.* **8**: 1.

Démoulin P, Aulanier G. 2010. Criteria for flux rope eruption: non-equilibrium versus torus instability. *Astrophys. J.* **718**: 1388.

Dungey JW. 1961. Interplanetary magnetic field and the auroral zones. *Phys. Rev. Lett.* **6**: 47.

Feynman J, Hundhausen AJ. 1994. Coronal mass ejections and major solar flares: the great active center of March 1989. *J. Geophys. Res., Space Phys.* **99**: 8451.

Forbes TG, Isenberg PA. 1991. A catastrophe mechanism for coronal mass ejections. *Astrophys. J.* **373**: 294.

Forbes TG, Linker JA, Chen J *et al.* 2006. CME theory and models. *Space Sci. Rev.* **123**: 251.

Gibb GPS, Mackay DH, Green LM *et al.* 2014. Simulating the formation of a sigmoidal flux rope in AR10977 from SOHO/MDI magnetograms. *Astrophys. J.* **782**: 71.

Gonzalez WD, Joselyn JA, Kamide Y *et al.* 1994. What is a geomagnetic storm? *J. Geophys. Res., Space Phys.* **99**: 5771.

Gonzalez WD, Echer E, Tsurutani BT *et al.* 2011. Interplanetary origin of intense, superintense and extreme geomagnetic storms. *Space Sci. Rev.* **158**: 69.

Gopalswamy N, Lara A, Lepping RP *et al.* 2000. Interplanetary acceleration of coronal mass ejections. *Geophys. Res. Lett.* **27**: 145.

Gosling JT. 1993. The solar flare myth. *J. Geophys. Res., Space Phys.* **98**: 18937.

Green LM, Kliem B. 2009. Flux rope formation preceding coronal mass ejection onset. *Astrophys. J. Lett.* **700**: L83.

Green LM, Kliem B. 2014. Observations of flux rope formation prior to coronal mass ejections, in *Nature of Prominences and their Role in Space Weather Proceedings of the International Astronomical Union, IAU Symposium* Volume 300. Schmieder B, Malherbe J-M, Wu ST (eds). pp 209–214. Cambridge University Press: Cambridge, UK and New York, NY.

Green LM, Kliem B, Wallace AJ. 2011. Photospheric flux cancellation and associated flux rope formation and eruption. *Astron. Astrophys.* **526**: A2.

Hood AW, Priest ER. 1981. Solar flares: Magnetohydrodynamic instabilities, in *Proceedings of the NATO Advanced Study Institutes Series*, Volume 68, Bonas, France, August 25–September 5, 1980. Bonnet RM, Dupree AK (eds). Springer Netherlands: Dordrecht, Netherlands, pp 509–531.

Illing RME, Hundhausen AJ. 1986. Disruption of a coronal streamer by an eruptive prominence and coronal mass ejection. *J. Geophys. Res., Space Phys.* **91**: 10951.

Jian L, Russell CT, Luhmann JG *et al.* 2006. Properties of interplanetary coronal mass ejections at one AU during 1995–2004. *Sol. Phys.* **239**: 393.

Klein LW, Burlaga LF. 1982. Interplanetary magnetic clouds at 1AU. *J. Geophys. Res., Space Phys.* **87**: 613.

Kliem B, Török T. 2006. Torus instability. *Phys. Rev. Lett.* **96**: 255002.

Lindsay GM, Luhmann JG, Russell CT *et al.* 1999. Relationships between coronal mass ejection speeds from coronagraph images and interplanetary characteristics of associated interplanetary coronal mass ejections. *J. Geophys. Res., Space Phys.* **104**: 12515.

Liu R, Liu C, Wang S *et al.* 2010. Sigmoid-to-flux-rope transition leading to a loop-like coronal mass ejection. *Astrophys. J. Lett.* **725**: L84.

Low BC. 1996. Solar activity and the corona. *Sol. Phys.* **167**: 217.

Mackay DH, van Ballegooijen AA. 2006. Models of the large-scale corona. I. Formation, evolution, and liftoff of magnetic flux ropes. *Astrophys. J.* **641**: 577.

Mackay DH, Green LM, van Ballegooijen A. 2011. Modeling the dispersal of an active region: quantifying energy input into the corona. *Astrophys. J.* **729**: 97.

Martin SF. 1980. Preflare conditions, changes and events. *Sol. Phys.* **68**: 217.

Owens M, Cargill P. 2004. Predictions of the arrival time of coronal mass ejections at 1AU: an analysis of the causes of errors. *Ann. Geophys.* **22**: 661.

Pulkkinen T. 2007. Space weather: terrestrial perspective. *Living Rev. Sol. Phys.* **4**: 1.

Russell CT, McPherron RL, Burton RK. 1974. On the cause of geomagnetic storms. *J. Geophys. Res., Space Phys.* **79**: 1105.

Savcheva A, van Ballegooijen AA. 2009. Nonlinear force-free modeling of a long-lasting coronal sigmoid. *Astrophys. J.* **703**: 1766.

Savcheva AS, Green LM, van Ballegooijen AA *et al.* 2012. Photospheric flux cancellation and the build-up of sigmoidal flux ropes on the Sun. *Astrophys. J.* **759**: 105.

Sheeley NR, Howard RA, Koomen MJ *et al.* 1982. Observations of coronal structure during sunspot maximum. *Space Sci. Rev.* **33**: 219.

Siscoe GL, Crooker NU, Elliott HA. 2006. Initial-condition influences on CME expansion and propagation. *Sol. Phys.* **239**: 293.

Steed K, Owen CJ, Démoulin P *et al.* 2011. Investigating the observational signatures of magnetic cloud substructure. *J. Geophys. Res., Space Phys.* **116**: 1106.

Su Y, van Ballegooijen A, Lites BW *et al.* 2009. Observations and nonlinear force-free field modeling of active region 10953. *Astrophys. J.* **691**: 105.

Svalgaard L. 1977. Geomagnetic activity: dependence on solar wind parameters, in *Coronal Holes and High Speed Wind Streams*. Zirker JB (ed.). Colorado Assoc. University Press: Boulder, CO, pp 371–441.

Tousey R. 1973. The solar corona, in *Space Research Conference*. Rycroft MJ, Runcorn SK (eds). Akademie-Verlag: Berlin, pp 713–730.

Tsurutani BT, Gonzalez WD, Lakhina GS *et al.* 2003. The extreme magnetic storm of 1–2 September 1859. *J. Geophys. Res.* **108**: 1268.

Valori G, Green LM, Démoulin P *et al.* 2012. Nonlinear force-free extrapolation of emerging flux with a global twist and serpentine fine structures. *Sol. Phys.* **278**: 73.

Watari S, Detman T. 1998. In situ local shock speed and transit shock speed. *Ann. Geophys.* **16**: 370.

Webb DF, Howard TA. 2012. Coronal mass ejections: observations. *Living Rev. Sol. Phys* **9**: 3.

Woo R, Armstrong JW, Sheeley NR *et al.* 1985. Doppler scintillation observations of interplanetary shocks within 0.3AU. *J. Geophys. Res., Space Phys.* **90**: 154.

Xie H, Gopalswamy N, St. Cyr OC *et al.* 2008. Effects of solar wind dynamic pressure and preconditioning on large geomagnetic storms. *Geophys. Res. Lett.* **35**: 6.

Zharkov S, Green LM, Matthews SA *et al.* 2011. February 15: Sunquakes produced by flux rope eruption. *Astrophys. J.* **741**: 35.

Correspondence to: Lucie Green

lucie.green@ucl.ac.uk

doi:10.1002/wea.2437